Charge correlations in the magnetoresistive oxide $La_{0.7}Ca_{0.3}MnO_3$ (invited)

J. W. Lynn[a] and C. P. Adams
NIST Center for Neutron Research, National Institute of Standards and Technology, Gaithersburg, Maryland 20899-8562 and Department of Physics, University of Maryland, College Park, Maryland 20742

Y. M. Mukovskii, A. A. Arsenov, and D. A. Shulyatev
Moscow Steel and Alloys Institute, Moscow 117936, Russia

Neutron scattering has been used to study the nature of the spin dynamics and charge correlations in a single crystal of the colossal magnetoresistive perovskite $La_{0.7}Ca_{0.3}MnO_3$. Diffuse scattering from lattice polarons develops as the Curie temperature is approached from below, along with short range polaron correlations that are consistent with stripe formation. Magnetic fields are found to suppress this polaron formation. The temperature dependence of the polaron correlations follows the same behavior as both the resistivity and the anomalous quasielastic component in the magnetic fluctuation spectrum, indicating that they have a common origin. © *2001 American Institute of Physics.* [DOI: 10.1063/1.1358331]

I. INTRODUCTION

The recent discovery of huge magnetoresistance effects in the manganese oxide class of materials[1] [such as $La_{1-x}A_xMnO_3$ (A=Sr, Ca, Ba)] has rekindled intense interest in these systems. In contrast to traditional isotropic ferromagnets such as Fe, Co, Ni, and EuO, where the spin system is isolated from the lattice, in the manganites the charge, spin, and lattice degrees of freedom are strongly coupled together, leading to a delicate balance of interactions that gives rise to a rich variety of physical phenomena of current interest in condensed matter physics. These include a metal–insulator transition concomitant with ferromagnetic ordering, charge and orbital ordering, polaron formation, electronic phase separation, and spin and charge stripes. The manganites are also related to the high T_C cuprate oxides, with a commonality of many of the materials properties and underlying physical concepts. Recent progress in our understanding of the cuprates has provided insights into the manganites, and a deeper understanding of the fundamental properties of the manganites will surely elucidate the shared concepts underlying both classes of materials. Finally, the colossal magnetoresistance (CMR) offers potential in a number of technologies, such as for read/write heads, sensors, and spin-polarized electronics, and this potential has also generated enormous interest.

Due to the similarity of the La and Ca ionic radii, the Ca system forms over the full compositional range, and the magnetic and structural properties of $La_{1-x}Ca_xMnO_3$ ($0 \leqslant x \leqslant 1$) were first characterized by Wollan and Koehler[2] and interpreted theoretically by Goodenough.[3] The undoped $LaMnO_3$ material is a Jahn–Teller distorted antiferromagnet, while doping produces a ferromagnetic regime ($0.15 < x < 0.5$) where CMR is observed. At half doping the system returns to an antiferromagnetic, charge-ordered insulator, and this basic behavior then extends to the fully substituted $CaMnO_3$, which is (undistorted) cubic. In the ferromagnetic regime the ground state spin dynamics for the Ca, Ba, and Sr-doped materials and related systems has a number of unusual properties such as large linewidths and anomalous dispersion,[4,5] while the combined metal–insulator and ferromagnetic transition has been found to be quite different from conventional isotropic ferromagnets.[6–9] In the Ca system in particular, the spin wave stiffness does not collapse as $T \rightarrow T_C$, but instead a quasielastic diffusive component develops in the excitation spectrum. Above T_C, the conductivity is characterized by hopping that is believed to be associated with polarons,[6,10–12] and recently direct evidence for the formation of lattice polarons has been observed in single crystals of the layered manganite $La_{1.2}Sr_{1.8}Mn_2O_7$,[13] in the cubic, half-doped $(Nd_{0.12}Sm_{0.88})_{0.52}Sr_{0.48}MnO_3$ material,[14] and in $La_{1-x}Ca_xMnO_3$.[15–17] For $La_{0.70}Ca_{0.30}MnO_3$ we find a direct relationship between the ferromagnetic transition and the polaron formation associated with the metal–insulator transition. In particular, we observe the formation of lattice polarons in the optimally doped cubic CMR material, and find clear evidence for polaron ordering in the paramagnetic phase that is consistent with stripe formation. More importantly, the temperature dependence of this polaron intensity develops simultaneously with the quasielastic spin fluctuation scattering, directly connecting these two phenomena with the resistivity.

II. EXPERIMENT

The sample is a 0.7 g single crystal grown by the floating zone technique,[18] with a single-peaked mosaic less than 0.25°. At this composition the crystal structure is orthorhombic, but the distortion is small and the domains are equally populated. Therefore for simplicity we will employ cubic notation ($a = 3.867$ Å at room temperature), where nearest-neighbor manganese atoms are along the [100]-type directions. Most measurements were taken in the $(hk0)$ plane on the BT-2 and BT-9 triple-axis spectrometers at NIST, using a variety of incident energies (13.7, 14.7, 30.5, and 50 meV) and collimations. For the unpolarized neutron measurements the monochromator and analyzer crystals were pyrolytic

[a]Author to whom correspondence should be addressed; electronic mail: jeff.lynn@nist.gov

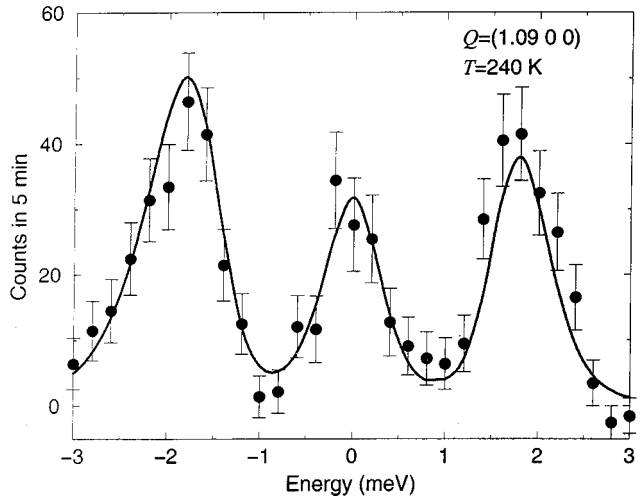

FIG. 1. Constant-**Q** scan taken at $T=240$ K, well below the Curie temperature of $T_C=257$ K, at a reduced wave vector of (0.09,0,0). The spin waves are observed in energy gain ($E<0$) and energy loss ($E>0$). In addition, a central quasielastic component to the fluctuation spectrum develops as $T \rightarrow T_C$.

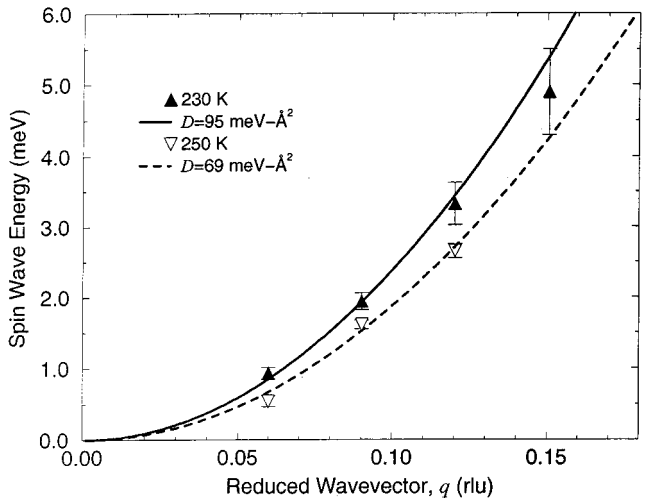

FIG. 2. Long wavelength spin wave dispersion along the (1,0,0) crystallographic direction (cubic notation) at two different temperatures. Solid curves are fits to Eq. (1). The data obey the quadratic relation, with a negligible gap in the spin wave spectrum.

graphite (PG), while for polarized beam measurements Heusler alloy polarizers were employed. PG filters were used when appropriate to suppress higher-order wavelength contaminations. Statistical uncertainties quoted represent 1 standard deviation.

III. RESULTS

A. Spin dynamics

A typical example of the magnetic fluctuation spectrum observed below the Curie temperature ($T_C=257$ K) is shown in Fig. 1, measured around the (1,0,0) reciprocal lattice vector. A q-independent nuclear incoherent scattering of 2.6 cts/min and a flat background of 1.6 have been subtracted from these data. At this reduced wave vector of (0.09,0,0) well defined spin wave excitations are observed in neutron energy gain ($E<0$) and energy loss ($E>0$), and the solid curve is a least-squares fit of the spin wave cross section, along with the quasielastic component centered at $E=0$, convoluted with the instrumental resolution. The magnetic excitations are conventional spin waves, with a dispersion relation given by (to leading order in q^2)

$$E=\Delta+D(T)q^2, \tag{1}$$

where Δ represents the spin wave energy gap, and the spin stiffness coefficient $D(T)$ is directly related to the exchange interactions. The spin wave gap Δ, which represents the energy to uniformly rotate the entire spin system away from the easy direction of magnetization, is much smaller than the exchange energies in the problem; Δ is too small ($\Delta<0.02$ meV) to be measured directly with neutrons anywhere in the metallic regime of these materials. This remarkable isotropy has been found for all these CMR ferromagnets, even for compositions close to the metal–insulator compositional transition.[16] Data taken at a series of qs reveal that the spin waves obey the quadratic dispersion law, as shown in Fig. 2.

The temperature dependence of the spin stiffness coefficient $D(T)$ obtained from such fits is shown in Fig. 3. The spin wave stiffness does not seem to collapse at the Curie temperature of $T_C=257(1)$ K, determined from measurements of the magnetic Bragg intensities. A well defined transition is observed, with no significant distribution of T_Cs in the sample.[15] Instead of the usual continuous softening of the spin wave spectrum, we see the development of the quasielastic component as shown in Fig. 1. The energy width of this scattering is quadratic in wave vector, with a spin diffusion constant $\Lambda=15(7)$ meV Å^2 (in this symmetry direction). The temperature evolution of this component is shown in Fig. 4 for three different wave vectors, where we see that the central component attains its maximum intensity close to T_C. The spin wave intensities, on the other hand, show a

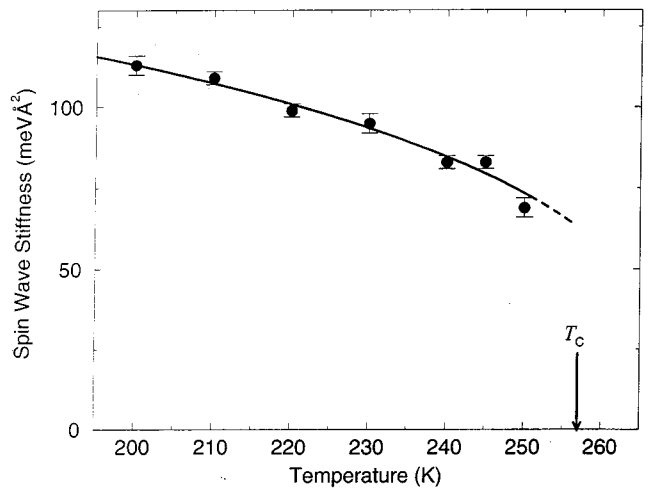

FIG. 3. Spin-wave stiffness coefficient $D(T)$ vs temperature obtained from data such as shown in Figs. 1 and 2. The spin waves do not appear to renormalize to zero at T_C, in contrast to the behavior of a conventional isotropic ferromagnet with a continuous (second order) magnetic phase transition.

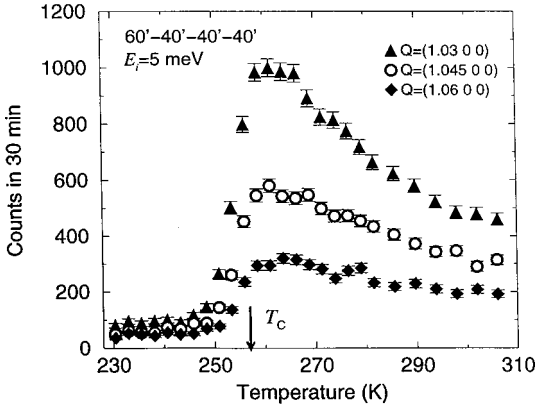

FIG. 4. Temperature dependence of the central component of the fluctuation spectrum, taken with high instrumental energy resolution, at three different reduced wave vectors. The central component peaks in intensity just above the Curie temperature of $T_C = 257$ K.

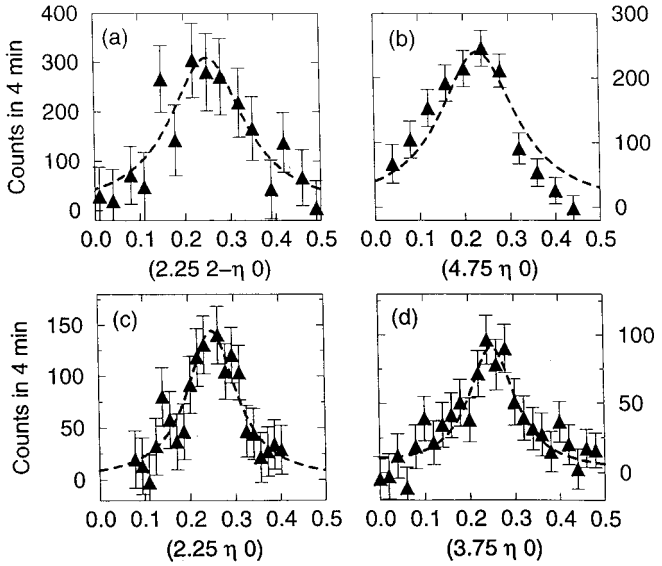

FIG. 5. Charge ordering satellites around different Bragg peaks. Measurements were taken above T_C between 270 and 280 K, with a background subtraction at 220 K. Peaks develop at $(\frac{1}{4},\frac{1}{4},0)$ positions relative to the Bragg peaks at: (a) (220), (b) (500), (c) (200), and (d) (400). All widths are larger than instrumental resolution and the dashed lines are Lorentzians.

decrease as the central component develops, rather than the usual increase of the Bose–Einstein population factor. Below T_C the quasielastic scattering is well separated from the spin wave contribution with this relatively good energy resolution (0.15 meV FWHM), while above T_C all the scattering is quasielastic. We find a length scale ~ 16 Å that is only weakly temperature dependent. This central peak, with the associated short length scale, has been interpreted as the spin component of polarons.[6,11] All these detailed results obtained on this high quality single crystal are in good overall agreement with previous measurements on polycrystalline samples,[6] as well as single crystal results on related $x = 1/3$ doped compounds.[7]

B. Polarons and polaron correlations

The scattering from a lattice polaron arises from the structural distortion that surrounds a carrier and traps it. Individual polarons generate diffuse (Huang) scattering around the fundamental Bragg peaks, and we observe such diffuse scattering in the present $La_{0.7}Ca_{0.3}MnO_3$ crystal, which is similar to the scattering from polaron distortions recently reported in the layered manganite $La_{1.2}Sr_{1.8}Mn_2O_7$,[13] and in the half-doped cubic $(Nd_{0.12}Sm_{0.88})_{0.52}Sr_{0.48}MnO_3$ material.[14] We also observe well-developed polaron–polaron correlations, which give rise to (short range) satellite peaks such as those shown in Fig. 5. These are scans of the elastic scattering measured around several nuclear Bragg peaks, and indicate commensurate polaron scattering with an ordering wave vector $(\frac{1}{4},\frac{1}{4},0)$ and equivalent directions. These polaron peaks have been observed around Bragg peaks such as the (2,0,0), (3,0,0), (5,0,0), (3,1,0), (4,2,0), and (2,2,0), while the intensity around the (0,0,0), (1,0,0), (1,1,0), and (2,1,0) was below our detection limit. This trend for the intensity to increase with increasing Q suggests that the dominant contribution to this scattering is from the lattice. This has been directly confirmed by polarized beam measurements, which show that the scattering in these peaks is dominated by the nonspin-flip (lattice) component. These charge peaks, both for $La_{0.7}Ca_{0.3}MnO_3$ as well as for the bilayer,[13] have a substantial intrinsic width, indicating that the polaron ordering is short range in nature. The width of the peaks is only weakly temperature dependent, and yields a correlation length of $\sim 10(2)$ Å (Fig. 5), which is the same basic length scale observed for the quasielastic magnetic scattering. The polaron peaks in both materials are also elastic, indicating that the polarons are static on a time scale of 1 ps. The polarons are surely hopping, though, and one of the interesting avenues to explore experimentally will be to investigate the nature of these peaks with much higher energy resolution, and in particular to determine if the observed q widths are related to the dynamics of the polarons instead of static short range order.[19]

The temperature dependence of the diffuse scattering associated with single polarons, measured at a wave vector of (1.85,2,0), is shown in Fig. 6 (solid triangles). The signal increases rapidly as the Curie temperature is approached from below as the polarons form, while above T_C we observe only a weak temperature dependence. This suggests that the number of polarons increases rapidly as $T \rightarrow T_C$, while above T_C the number is roughly constant. The temperature dependence of the intensity of the satellite peak at (3.75,0.25,0) is also shown in Fig. 6 (open circles). We see that the scattering begins to develop in this sample ~ 30 K below T_C, rapidly develops as $T \rightarrow T_C$, and peaks just above the ordering temperature. This behavior is very similar to the temperature dependence of the quasielastic component of the spin fluctuation spectrum, as well as the resistivity,[15] indicating that they all have a common origin. Finally, we note that the intensity of the polaron satellite peaks decreases with increasing field as shown in Fig. 7. Thus the polarons ''melt'' when the magnetization develops and the conductivity increases, either by lowering the temperature or increasing the applied field. Identical behavior has been observed both for the central component of the fluctuation spectrum,[6] as well as the polaron peaks in the bilayer system.[13]

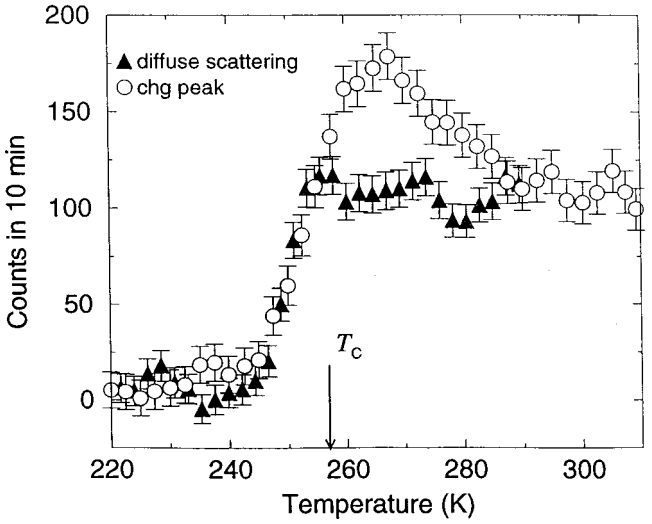

FIG. 6. Temperature dependence of the neutron intensity for the polaron peaks in $La_{0.7}Ca_{0.3}MnO_3$ (open circles), showing that the scattering increases with decreasing temperature until the ferromagnetic transition temperature is reached, and then the scattering decreases rapidly as the charges ''melt'' and the system becomes a ferromagnetic metal. Also shown is the temperature dependence of the intensity of the diffuse scattering at a wave vector of (1.85,2,0) near a fundamental Bragg reflection, which reflects the scattering from individual polarons. The signal increases rapidly as the Curie temperature is approached from below as the polarons form, while above T_C we observe only a weak temperature dependence. This suggests that the number of polarons increases rapidly as $T \rightarrow T_C$, while above T_C the number is roughly constant.

A familiar model that can explain both the ordering wave vector of $(\frac{1}{4},\frac{1}{4},0)$ for the lattice polaron scattering as well as the overall behavior of the observed intensities of the short-range correlation peaks is the CE model developed for the half-doped case.[3] The CE model has an orbitally ordered Jahn–Teller lattice with charge stripes in the [110] direction. Such ordering has been observed for $x \geqslant \frac{1}{2}$, with the lattice

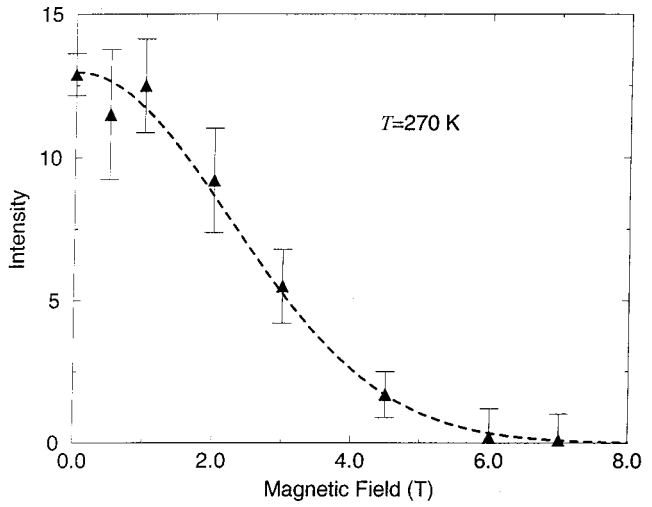

FIG. 7. Field dependence of the intensity of the polaron–polaron correlation peaks, showing that the intensity decreases with increasing field. Thus the polarons ''melt'' when the magnetization develops and the conductivity increases, either by lowering the temperature or by increasing the applied field.

and antiferromagnetic ordering at low temperatures.[20] This contrasts with the present ferromagnetic system, where the orbital/charge correlations are short range in nature and occur only *above* T_C. The CE model would of course need to be modified to accommodate the smaller doping level, and recent work indicates that the ordering wave vector does not depend strongly on doping.[17] The CE model also has an antiferromagnetic ground state, but in the present system we do not find any evidence of antiferromagnetic correlations.

Stripe formation has been observed in the related cuprates and nickelates, but the intrinsic magnetism in those systems is always antiferromagnetic in nature. This gives rise to separate satellite peaks associated with the charge and spin order.[21,22] We have found no evidence for separate magnetic satellites in $La_{0.7}Ca_{0.3}MnO_3$, which is not surprising in this ferromagnetic system where the spin stripes would be expected to give a contribution at the same satellite positions as the charge satellites. It might then seem surprising that we observe no significant magnetic component to the satellite peaks. However, the nature of the two types of scattering is quite different. The charge scattering originates from well-formed (static, on this time scale) Jahn–Teller distorted MnO_6 octahedra, which then form a ''stripe'' structure with a correlation length of ~ 10 Å. The spin part of this structure would have the same short correlation length, but the magnetic scattering itself has a short correlation range of only ~ 15 Å. Model calculations then show that the combination of the two short correlation ranges renders the spin polaron–polaron correlation scattering too weak to be observed at any of the satellite positions. We conclude then that the scattering of the lattice component of the polarons occurs around the high-Q fundamental Bragg peaks, along with the broad satellite peaks associated with polaron–polaron correlations, while the dominant magnetic contribution occurs around the low-Q fundamental Bragg reflections, in the form of the quasielastic scattering.

The above experimental results reveal that both the spin and charge correlations associated with the polarons in $La_{0.7}Ca_{0.3}MnO_3$ appear together, and have a very similar spatial and temperature dependence. The metal–insulator crossover in the conductivity also occurs close to T_C. This coincidence may explain the amplified magnetoresistive effects, as well as the absence of conventional magnetic critical behavior, both in the Ca-doped system as well as in other materials.[7] This behavior is not universal, however. In the higher T_C Sr and Ba systems, for example, the polaron formation[5,8,23] and conductivity crossover[24] can occur at temperatures substantially higher than the Curie point, reducing the magnetoresistive effects and rendering the spin dynamics and ferromagnetic phase transition more conventional.[25]

Our original interpretation of the anomalous magnetic properties of the Ca-doped system was that it was inhomogeneous at elevated temperatures, consisting of two distinct phases.[6] The preferred phase at low T (or high field) is an ordered ferromagnet with metallic conductivity, a finite magnetization, and well-defined spin waves, while the high-T phase is a paramagnet where the electrons diffuse on a short length scale. We have found additional evidence for this

phase separation scenario[26] in measurements of long equilibration times near T_C, as well as in the behavior of the transition upon oxygen isotope substitution,[27] and this behavior appears to be dictated by the polaron formation. The physical quantities that control the characteristic temperature for polaron formation, including the role that metallurgical defects play in their formation, still remain to be elucidated. These charge-ordered phases represent one of the most intriguing results of balancing the spin, lattice, and electronic degrees of freedom, and will no doubt continue to attract considerable interest.

ACKNOWLEDGMENTS

Research at the University of Maryland is supported by the NSF, Grant No. DMR 97-01339 and NSF-MRSEC, Grant No. DMR 00-80008. The work in Moscow was supported by ISTC Grant No. 636.

[1] R. von Helmolt, J. Wecker, B. Holzapfel, L. Schultz, and K. Samwer, Phys. Rev. Lett. **71**, 2331 (1993); S. Jin, T. H. Tiefel, M. McCormack, R. A. Fastnacht, R. Ramesh, and L. H. Chen, Science **264**, 413 (1994).
[2] E. O. Wollan and W. C. Koehler, Phys. Rev. **100**, 545 (1955); For a recent experimental review see A. P. Ramirez, J. Phys.: Condens. Matter **9**, 8171 (1997).
[3] J. B. Goodenough, Phys. Rev. **100**, 564 (1955).
[4] H. Y. Hwang, P. Dai, S.-W. Cheong, G. Aeppli, D. A. Tennant, and H. A. Mook, Phys. Rev. Lett. **80**, 1316 (1998).
[5] L. Vasiliu-Doloc, J. W. Lynn, A. H. Moudden, A. M. de Leon-Guevara, and A. Revcolevschi, Phys. Rev. B **58**, 14913 (1998).
[6] J. W. Lynn, R. W. Erwin, J. A. Borchers, Q. Huang, A. Santoro, J.-L. Peng, and Z. Y. Li, Phys. Rev. Lett. **76**, 4046 (1996); J. W. Lynn, R. W. Erwin, J. A. Borchers, A. Santoro, Q. Huang, J.-L. Peng, and R. L. Greene, J. Appl. Phys. **81**, 5488 (1997).
[7] J. A. Fernandez-Baca, P. Dai, H. Y. Hwang, C. Kloc, and S.-W. Cheong, Phys. Rev. Lett. **80**, 4012 (1998).
[8] L. Vasiliu-Doloc, J. W. Lynn, A. H. Moudden, A. M. de Leon-Guevara, and A. Revcolevschi, J. Appl. Phys. **81**, 5491 (1997).
[9] J. J. Rhyne, H. Kaiser, H. Luo, G. Xiao, and M. L. Gardel, J. Appl. Phys. **83**, 7339 (1998).
[10] S. J. L. Billinge, R. G. DiFrancesco, G. H. Kwei, J. J. Neumeier, and J. D. Thompson, Phys. Rev. Lett. **77**, 715 (1996); D. Louca, T. Egami, E. L. Brosha, H. Röder, and A. R. Bishop, Phys. Rev. B **56**, 8475 (1997).
[11] J. M. deTeresa, M. R. Ibarra, P. A. Algarabel, C. Ritter, C. Marquina, J. Blasco, J. Garcia, A. del Moral, and Z. Arnold, Nature (London) **386**, 256 (1997).
[12] For a review, see A. S. Alexandrov and N. F. Mott, *Polarons and Bipolarons* (World Scientific, Singapore, 1995).
[13] L. Vasiliu-Doloc *et al.*, Phys. Rev. Lett. **83**, 4393 (1999).
[14] S. Shimomura, N. Wakabayashi, H. Kuwahara, and Y. Tokura, Phys. Rev. Lett. **83**, 4389 (1999).
[15] C. P. Adams, J. W. Lynn, Y. M. Mukovskii, A. A. Arsenov, and D. A. Shulyatev, Phys. Rev. Lett. **85**, 3954 (2000).
[16] For a review see J. W. Lynn, J. Superconductivity Novel Magnetism **13**, 263 (2000).
[17] P. Dai, J. A. Fernandez-Baca, N. Wakabayashi, E. W. Plummer, Y. Tomioka, and Y. Tokura, Phys. Rev. Lett. **85**, 2553 (2000).
[18] D. Shulyatev, S. Karabashev, A. Arsenov, and Y. Mukovskii, J. Cryst. Growth **199**, 511 (1999).
[19] G. M. Zhao, K. Conder, H. Keller, and K. A. Müller, Nature (London) **381**, 676 (1996).
[20] S. Mori, C. H. Chen, and S.-W. Cheong, Nature (London) **392**, 473 (1998); Phys. Rev. Lett. **81**, 3972 (1998); K. H. Kim, M. Uchara, and S.-W. Cheong, Phys. Rev. B **62**, R11945 (2000).
[21] J. M. Tranquada, D. J. Buttrey, V. Sachan, and J. E. Lorenzo, Phys. Rev. Lett. **73**, 1003 (1994).
[22] S.-H. Lee and S.-W. Cheong, Phys. Rev. Lett. **79**, 2514 (1997).
[23] J. W. Lynn, L. Vasiliu-Doloc, K. Ghosh, G.-m. Zhao, V. Smolyaninova, R. L. Greene, S. N. Barilo, G. L. Bychkov, and L. A. Kurnevitch (preprint).
[24] A. Urushibara, Y. Moritomo, T. Arima, A. Asamitsu, G. Kido, and Y. Tokura, Phys. Rev. B **51**, 14 (1995); **51**, 103 (1995); A. Anane, C. Dupas, K. Le Dang, J. P. Renard, P. Veillet, A. M. de Leon-Guevara, F. Millot, L. Pinsard, and A. Revcolevschi, J. Phys.: Condens. Matter **7**, 7015 (1995).
[25] K. Ghosh, C. J. Lobb, R. L. Greene, S. G. Karabashev, D. A. Shulyatev, A. A. Arsenov, and Y. Mukovskii, Phys. Rev. Lett. **81**, 4740 (1998).
[26] A. Moreo, S. Yunoki, and E. Dagotto, Science **283**, 2034 (1999).
[27] C. P. Adams, J. W. Lynn, V. Smolyaninova, R. L. Greene, W. Ratcliffe II, and S.-W. Cheong (preprint).